Effect of spontaneous polarization and polar surface anchoring on the director and layer structure in surface-stabilized ferroelectric liquid crystal cells

Nataša Vaupotič[1,3] and Martin Čopič[2,3]
[1]*Department of Physics, Faculty of Education, University of Maribor, Koroška 160, 2000 Maribor, Slovenia*
[2]*Department of Physics, Faculty of Mathematics and Physics, University of Ljubljana, Jadranska 19, 1000 Ljubljana, Slovenia*
[3]*Jožef Stefan Institute, Jamova 39, 1000 Ljubljana, Slovenia*
(Received 14 August 2003; published 31 December 2003)

We use the Landau–de Gennes model to study theoretically the effect of the magnitude of the spontaneous polarization (P_S), the ratio (r) between the equilibrium layer tilt and the smectic cone angle, the thickness of the insulating alignment layers and the strength of the polar and nonpolar surface anchoring on the director and layer structure in surface-stabilized ferroelectric liquid crystal cells with the chevron structure of smectic layers. The system shows a surprising number of stable structures, accompanied by one or two metastable ones. At P_S greater than the critical value only quasimonostable structures, which can exhibit the thresholdless (V-shaped) switching, exist at all r and both at weak and strong polar surface anchoring. At lower P_S bistable and monostable structures can coexist. Bistable structures can be expected at high r, low P_S and if polar surface anchoring is weaker than the nonpolar one. Lowering the ratio r and/or increasing the strength of polar anchoring promotes the stability of monostable structures. Thicker insulating alignment layers also drive the system into the monostable state. Polar surface anchoring induces a large surface electroclinic effect. As a result the nematic deformations close to the surfaces are very strong and the stress is relieved by bending of the smectic layers. This leads to the formation of a double chevron structure which is stable at very large polar anchoring and due to the surface electroclinic effect it is metastable also at lower values of polar anchoring.

DOI: 10.1103/PhysRevE.68.061705 PACS number(s): 61.30.Dk, 61.30.Hn, 61.30.Gd, 42.79.Kr

I. INTRODUCTION

The chevron structure (Fig. 1) of the smectic layers is a well known characteristic of most surface-stabilized cells filled with ferroelectric smectic-$C^\star$ liquid crystal [1,2]. These cells in general exhibit two stable director states. They can be switched between them by an external voltage applied to the cell. Switching occurs only at fields stronger than the threshold field because the director rotation is accompanied by a significant increase in the elastic energy around the chevron tip [3]. The bistability of such cells does not allow the realization of the gray scale. The latter requires thresholdless switching, the mechanism of which is still under discussion. It is also debated whether thresholdless switching is an intrinsic [4] or an apparent [5] phenomenon. At first thresholdless switching has been attributed to antiferroelectricity in planar smectic liquid crystal cells [6]. In theoretical modeling the V-shaped switching was related to strong polar anchoring of the antiferroelectric liquid crystal to polymer aligning layers [7,8]. However, it has recently been shown that the V-shaped switching is a feature of the surface-stabilized ferroelectric liquid crystal (SSFLC) cells [9], that it is of the electrostatic origin [10], and that the reorientation of the optic axis is due to the director rotation on the smectic cone [9,11]. In cells filled with materials with high spontaneous polarization, monostable structures can be expected due to the polarization self-interaction, accompanied by the strong surface anchoring and the influence of the insulating alignment layer. The phenomenon has recently been considered theoretically [12] in a bookshelf geometry of the smectic layers. The bookshelf geometry is a reasonable first approximation since the layer tilt angle in such cells is usually much smaller than the optical tilt angle.

In the present work we extend the study of Čopič *et al.* [12] to the SSFLC cells with a chevron structure of smectic layers. We study theoretically the effect of the magnitude of the spontaneous polarization, the ratio between the equilibrium layer tilt and the smectic cone angle, the thickness of the insulating alignment layers, and the strength of the polar and nonpolar surface anchoring on the director and layer structure in such cells. We use the model put forward by the present authors and co-workers [13] and modify it so that it

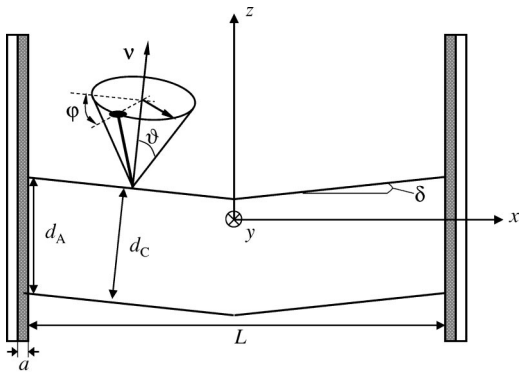

FIG. 1. The chevron structure in a SSFLC cell. L is the cell thickness, a is the thickness of the insulating alignment layer, d_A is the smectic layer thickness in the smectic-A phase, d_C is the smectic layer thickness in the bulk smectic-C^*, ν is the direction of the normal to the smectic layer, δ is the smectic layer tilt, ϑ is the cone angle, φ determines the director position on the smectic cone. The nematic director is presented by the thick line with a circle at the end. The arrow presents the direction of the spontaneous polarization.

 ©2003 The American Physical Society

is applicable to the systems with spontaneous polarization and varying ratio between the equilibrium layer tilt and the smectic cone angle. The model is presented in Sec. II together with a short insight into the numerical calculations. In Sec. III we discuss qualitatively the competing effects which determine the director and layer structure. Due to the numerous competing effects we predict a number of possible structures which are subsequently obtained by the numerical analysis, the results of which are presented in Sec. IV. Finally, in Sec. V we draw some brief conclusions.

II. MODEL

The geometrical model of the cell structure is shown in Fig. 1. The cell of thickness L is formed by two conducting electrodes that are separated from the liquid crystal by an insulating alignment layer of thickness a. The electrodes lie in the yz plane. The smectic layer thickness required by the surface is d_A, the layer thickness preferred by the bulk smectic-$C^\star$ is d_C. The smectic layer normal is denoted by $\boldsymbol{\nu}$, $\mathbf{n}$ is the director, ϑ is the smectic cone angle and the angle φ determines the director position on the cone. Structure with no director tilt in the y direction is monostable. In general the director is tilted in the y direction and the structure is bistable. In the figure the director is tilted in the y direction, however the structure with the tilt in the positive y direction is also possible. The ferroelectric polarization $\mathbf{P}$ is perpendicular to the layer normal and the director, $\mathbf{P}=P_0\boldsymbol{\nu}\times\mathbf{n}$, where $P_S=P_0\sin\vartheta_B$ is the magnitude of the spontaneous polarization in the bulk liquid crystal. We assume that all variables are functions of the coordinate x only.

The free energy consists of the bulk and surface contributions. The bulk free energy density f consists of the nematic f_n, smectic f_s and electrostatic f_e contributions. In a one-constant K nematic approximation the nematic contribution is

$$f_n=\frac{1}{2}K([\boldsymbol{\nabla}\cdot\mathbf{n}]^2+(\boldsymbol{\nabla}\times\mathbf{n})^2).$$

The smectic contribution to the free energy density [13] is expressed in terms of the nematic director and the complex smectic order parameter ψ,

$$f_s=c_{||}|(\mathbf{n}\cdot\boldsymbol{\nabla}-iq_0)\psi|^2+c_\perp|\mathbf{n}\times\boldsymbol{\nabla}\psi|^2+D|(\mathbf{n}\times\boldsymbol{\nabla})^2\psi|^2. \tag{1}$$

The complex smectic order parameter ψ is spatially dependent,

$$\psi(\mathbf{r})=\eta_B\exp(i\phi(\mathbf{r})),$$

where η_B is the magnitude of the smectic order parameter which we assume to be constant and equal to its value in bulk smectic-$C^\star$. The phase factor $\phi(\mathbf{r})$ determines the position of smectic layers. The smectic layer normal is defined as $\boldsymbol{\nu}=\boldsymbol{\nabla}\phi(\mathbf{r})/|\boldsymbol{\nabla}\phi(\mathbf{r})|$.

The parameters $c_{||}$, $c_\perp$, and D in Eq. (1) are related to the smectic elastic constants. The de Gennes smectic layer compressibility elastic constant B is related to $c_{||}$ as $B=c_{||}q_0^2\eta_B^2$ [13]. The parameter $c_\perp$ is temperature dependent. It is positive in the smectic-A phase and it is negative in the smectic-$C^\star$ phase. The parameter q_0 has to be chosen such that the compressibility term in the smectic free energy density [the first term in Eq. (1)] is zero both in the bulk smectic-A phase and in the successive smectic-$C^\star$ phase. In the bulk smectic-A phase the director is parallel to the smectic layer normal and the compressibility term is zero if the layer thickness equals d_A. In the bulk smectic-$C^\star$ phase the director tilt with respect to the layer normal is $\vartheta_B=\arctan\sqrt{|c_\perp|/(2Dq_0^2)}$ [13]. In general, the layer thickness in the smectic-$C^\star$ phase is

$$d_C=d_A\cos r\vartheta_B, \tag{2}$$

where the value of the parameter r is between 0 and 1. If $r=0$, the material is called an ideal de Vries material in which there is no layer shrinkage at the transition from the smectic-A to the smectic-$C^\star$ phase. If $r=1$, we describe a material with $d_C=d_A\cos\vartheta_B$. In our previous work we have considered only the latter materials. Although the most common values of r are between 0.8 and 0.9, the approximation $r=1$ allowed us to describe most of the important characteristics of the surface stabilized smectic-C cells with a chevron structure. However, in materials which exhibit thresholdless switching r is usually closer to 0 than 1 and for a typical material like W415 [14] it is ≈ 0.2.

To meet all the above mentioned requirements for the compressibility term we choose

$$q_0=q_A\frac{\cos\vartheta_B}{\cos r\vartheta_B}, \tag{3}$$

where $q_A=2\pi/d_A$. In the bulk smectic-$C^\star$ in which the layers run along the z direction, we can express $\phi(\mathbf{r})=2\pi z/d_C$ and $\mathbf{n}=(0,\sin\vartheta_B,\cos\vartheta_B)$. It is then straightforward to show that the compressibility term in Eq. (1) is zero if the condition (2) is satisfied.

In SSFLC cells the equilibrium layer tilt angle (δ_E) is such that the smectic layer thickness at the surface is d_A and inside the cell it is d_C. It is easily seen that $\delta_E=r\vartheta_B$, so in the chevron geometry the parameter r presents the ratio between the equilibrium layer tilt and the bulk value of the smectic cone angle.

The total electric field inside the liquid crystal consists of the field due to the surface charge at the electrodes (this we call the external electric field), the electric field in the insulating alignment layers and the electric field due to the spatially varying polarization inside liquid crystal. Since the ferroelectric polarization is a function of the x-coordinate only, the resulting electric field has a component along the x-axis only, $E_P=-P_x/(\varepsilon\varepsilon_0)$, where P_x is the x component of the spontaneous polarization. The external electric field also points along the x direction and its magnitude is $E_{ext}=\sigma/(\varepsilon\varepsilon_0)$, where σ is the surface charge density on the electrodes. The electric field strength inside the insulating alignment layer of thickness a is $E_{diel}=\sigma/(\varepsilon\varepsilon_0)$. We have assumed an isotropic dielectric tensor and that the dielectric strengths of the insulating alignment layer and the liquid crystal are the same. If different dielectric strengths were

chosen for the liquid crystal and the insulating alignment layers this would merely change the effective thickness of the insulating alignment layers.

The electrostatic contribution to the free energy density is [12]

$$f_e=\frac{1}{2}\varepsilon\varepsilon_0 E_{ext}^2+\frac{P_x^2}{2\varepsilon\varepsilon_0}-P_x E_{ext}. \tag{4}$$

The first term is the free energy density due to the induced dipoles, the second term presents the self-electrostatic energy due to the spatial variation of the spontaneous polarization, and the third term is the interaction of the spontaneous polarization with the external electric field. Since we have a voltage V applied to the surface electrodes, the internal electric field is such that

$$-\frac{\sigma L}{\varepsilon\varepsilon_0}-\frac{2\sigma a}{\varepsilon\varepsilon_0}+\int_{-L/2}^{L/2}\frac{P_x dx}{\varepsilon\varepsilon_0}=V.$$

We thus see that even if the voltage applied to the cell is zero there is a net surface charge

$$\sigma=\frac{1}{L+2a}\int_{-L/2}^{L/2}P_x dx \tag{5}$$

at the electrodes to compensate for the electric field due to the divergence of the spontaneous polarization.

The director and layer structure inside the cell essentially depends on the surface anchoring. We consider a combination of polar and nonpolar surface anchoring,

$$F_{surf}=-\frac{1}{2}W_{np}(\sin^2\varphi)_{x=\pm L/2}\pm W_p\left(\frac{\mathbf{P}\cdot\hat{\mathbf{x}}}{P_S}\right)_{x=\pm L/2}, \tag{6}$$

where W_{np} is the strength of the nonpolar surface anchoring which, at $W_{np}>0$, prefers $\varphi=\pm\pi/2$ at the surfaces, and the polar anchoring is chosen such that at $W_p>0$ it prefers the polarization at the surface being perpendicular to the surface ($\hat{\mathbf{x}}$ is the unit vector in the x direction, i.e., perpendicular to the surface) and pointing inside the cell. The polar anchoring is also sensitive to the magnitude of the spontaneous polarization. Surface energy decreases with larger P_S. The polarity of the surface thus forces the increase in the cone angle ϑ in order to increase P_S. This is the surface electroclinic effect [15] and experiments in the smectic-A phase of the W415 [14] show that it can be very large.

With the chosen surface anchoring the surface is bistable. Let us consider the function

$$f(\varphi)=-\frac{1}{2}W_{np}\sin^2\varphi+W_p\sin\varphi,$$

which represents the energy due to the surface anchoring at the left surface in the case of polar anchoring which is independent of the magnitude of the spontaneous polarization. Until $W_p<W_{np}$ the energy $f(\varphi)$ has two minima: at $\varphi=\pi/2$ and $\varphi=-\pi/2$. At $W_p>W_{np}$ there is only one minimum at $\varphi=-\pi/2$. It is similar at the right surface. At $W_p<W_{np}$ there are two minima and at $W_p>W_{np}$ there is only one minimum at $\varphi=\pi/2$. So if polar anchoring is stronger than nonpolar anchoring one can expect only one stable structure and at lower polar anchoring two different structures can coexist (e.g., one monostable and one bistable).

We also note that the chevron tip can be regarded as an internal surface with nonpolar surface anchoring because in order to reduce the nematic deformations around the chevron tip $\varphi=\pm\pi/2$ is preferred around the chevron tip as will be discussed in more detail in Sec. III.

Numerical calculations

The numerical calculations are performed in the xyz coordinate system. The director is expressed by its components along the x, y, and z axes. The director is a function of the x-coordinate only,

$$\mathbf{n}(x)=(k(x),l(x),m(x)), \tag{7}$$

where $m=(1-k^2-l^2)^{1/2}$, because $|\mathbf{n}(x)|=1$. The smectic order parameter phase factor is

$$\phi(x,z)=q_A(z-u(x)).$$

The layer displacement field $u(x)$ describes the departure from the planar layer configuration. The variables used in calculations are thus $k(x)$, $l(x)$, and $u(x)$.

The equilibrium structure is found by minimizing the bulk free energy, taking into account the specific boundary conditions. Here we should mention that the inclusion of the polar surface anchoring significantly complicates the calculation. In studying the symmetric chevron structures [3,13] we were solving a set of three coupled differential equations that were of the second order. The Euler-Lagrange equations that follow from the minimization of the free energy are actually of the fourth order in $u(x)$ since there are second order derivatives of $u(x)$ in the smectic free energy density. The variable $u(x)$ itself does not enter the free energy, only its spatial derivative. So we could minimize the free energy with respect to $du(x)/dx$. The boundary condition of the layer displacement being zero at the surface is satisfied automatically in a symmetric chevron because $du(x)/dx$ is antisymmetric around the chevron tip. In a nonsymmetric chevron we can still minimize the free energy with respect to $du(x)/dx$, but in addition we have to fulfill an integral condition for u,

$$\int_{-L/2}^{L/2}\frac{du}{dx}dx=0.$$

A different procedure can be chosen. One can work with $u(x)$ and a fourth order differential equation, but a simple boundary condition of the displacement being zero at the surfaces,

$$u(x=\pm L/2)=0. \tag{8}$$

We have chosen the latter way.

For computational purposes we express the free energy in a dimensionless form. We introduce the following dimensionless variables:

$$\xi = x/L, \quad \tilde{u}(\xi) = u(x)/L,$$

parameters:

$$\tilde{\sigma} = \frac{\sigma \sin \vartheta_B}{P_S}, \quad C_R = \frac{c_{||}}{|c_\perp|}, \quad \gamma_{p,np} = \frac{W_{p,np} L}{K}, \quad \tilde{a} = a/L$$

and characteristic lengths:

$$\lambda_{||} = \sqrt{\frac{K}{B}}, \quad k_{||} = \frac{\lambda_{||}^2}{L^2},$$

$$\lambda_{ch} = \sqrt{\frac{2D}{|c_\perp|}} = (q_0 \tan_B)^{-1}, \quad k_{ch} = \frac{\lambda_{ch}^2}{L^2},$$

$$\lambda_S = \sqrt{\frac{\varepsilon \varepsilon_0 K}{P_S^2}}, \quad k_S = \frac{\lambda_S^2}{L^2}.$$

With this choice of parameters the magnitude of the spontaneous polarization P_S acts as a scaling parameter. The characteristic length λ_S presents the thickness of the deformed layer at the surfaces when the surface and the bulk conditions dictate different orientation of polarization than the electrostatic energy. The parameter k_S we call the stiffness parameter and it is a measure for the relative thickness of this surface deformed layer. The characteristic length $\lambda_{||}$ is the smectic penetration depth and it is of the same order of magnitude as d_A and the characteristic width of the chevron tip λ_{ch}.

The dimensionless free energy G is the sum of the bulk G_B and the surface G_A contribution. The bulk contribution is

$$G_B = \int_{-1/2}^{1/2} \left\{ \frac{1}{2}(k_\xi^2 + l_\xi^2 + m_\xi^2) + \frac{1}{k_{||}} \mathcal{A}^2 \right\} d\xi + \frac{k_{ch}}{k_{||} C_R} \int_{-1/2}^{1/2} \left\{ \frac{1}{2} \tilde{u}_{\xi\xi}^2 - \frac{1}{k_{ch}} \mathcal{B} + \frac{1}{2} L^2 q_A^2 \mathcal{B}^2 \right\} d\xi + \frac{1}{2 k_S \sin^2 \vartheta_B} \int_{-1/2}^{1/2} \left\{ \frac{l^2}{1+\tilde{u}_\xi^2} + \tilde{\sigma}^2 + \frac{2 l \tilde{\sigma}}{\sqrt{1+\tilde{u}_\xi^2}} \right\} d\xi, \tag{9}$$

with

$$\mathcal{A} = -\tilde{u}_\xi k + m - \frac{\cos \vartheta_B}{\cos r \vartheta_B},$$

$$\mathcal{B} = l^2 (1 + \tilde{u}_\xi^2) + (m \tilde{u}_\xi + k)^2$$

and the indices ξ denote derivatives with respect to ξ. From Eq. (9) we see that when $k_S \sin^2 \vartheta_B$ is of the same order of magnitude as $k_{||}$ or k_{ch}, the electrostatic contribution to the free energy is of the same order as the nematic and smectic contributions. So monostable structures can be expected to be stable at $k_S \sin^2 \vartheta_B < k_{ch,||}$.

The surface contribution is

$$G_{surf} = \mp \frac{\gamma_p}{\sin^2 \vartheta_B} \left(\frac{l}{\sqrt{1+\tilde{u}_\xi^2}} \right)_{\xi = \pm 1/2} - \frac{\gamma_{np}}{2} (\sin^2 \varphi)_{\xi = \pm 1/2},$$

where $\sin \varphi = l / \sin \vartheta$ and $\cos \vartheta = (m - k\tilde{u}_\xi)/\sqrt{1+\tilde{u}_\xi^2}$.

Minimization of the free energy gives three Euler-Lagrange equations and three boundary conditions [in addition to the boundary condition (8)]. The free energy [Eq. (9)] has to be minimized such that the condition (5) is satisfied. In a dimensionless form this condition is

$$\tilde{\sigma} = -\frac{1}{1+2\tilde{a}} \int_{-1/2}^{1/2} \frac{l}{\sqrt{1+\tilde{u}_\xi^2}} d\xi. \tag{10}$$

The Euler-Lagrange equations are solved numerically using the relaxation method [16]. After each cycle, when corrected values to the variables are found, new $\tilde{\sigma}$ is calculated from Eq. (10) and is used in the succeeding cycle.

We study the director and layer structure inside the cell as a function of the stiffness parameter k_S, the parameter $r = \delta_E / \vartheta_B$, and the magnitude of the polar and nonpolar surface anchoring. As a common set of parameters we choose: $L = 2$ μm, $\varepsilon = 10$, $C_R = 10$, $d_A = 5$ nm, $a = 10$ nm, $B = 10^5$ J/m^3, $K = 4 \times 10^{-12}$ J/m, and $\vartheta_B = 30°$. With this set of parameters $k_{||} = 10^{-5}$. If $r = 0.2$ and $P_S = 300$ nC/cm^2 (typical values for W415) then $k_{ch} = 2.5 \times 10^{-5}$ and $k_S = 10^{-5}$.

III. COMPETING INTERACTIONS IN SSFLC CELLS

In this section we discuss the effects that determine the layer and director structure in SSFLC cells. We also introduce the terminology used to name different structures.

The chevron geometry of the smectic layers is a result of the competition between the surface memory effect (the layers are strongly anchored at the surface in the preceding smectic-*A* phase [17]) and the natural smectic-*C** layer thickness. At the chevron tip the smectic layers are dilated and the cone angle is reduced [13]. To reduce the nematic deformation the director at the chevron tip tilts in the *yz* plane ($\varphi = \pm \pi/2$ at the chevron tip). At low spontaneous polarization and low polar surface anchoring the director position on the cone on both sides of the chevron tip is approximately uniform [solid line in Fig. 2(a)]. This is a common uniform bistable structure and we denote it by *B*. At stronger polar anchoring one side of the cell remains approximately uniform and the other side is splayed [dashed line in Fig. 2(a)]. One half of the cell is splayed only if the ratio $r = \delta_E / \vartheta_B$ is high enough. At low values of r the whole cell is splayed [solid line in Fig. 2(b)]. We shall call such a structure the *S* structure, to distinguish between the structures with $\varphi = \pm \pi/2$ at the chevron tip (*B*) and the structures with $\varphi \approx 0$ at the chevron tip (*S*).

The internal electric field due to the polarization charge induced by the spontaneous polarization can have a significant effect on the director and layer structures. This has already been recognized by Nakagawa and Akahane [18] in the bookshelf geometry. Sabater and co-workers [19] considered

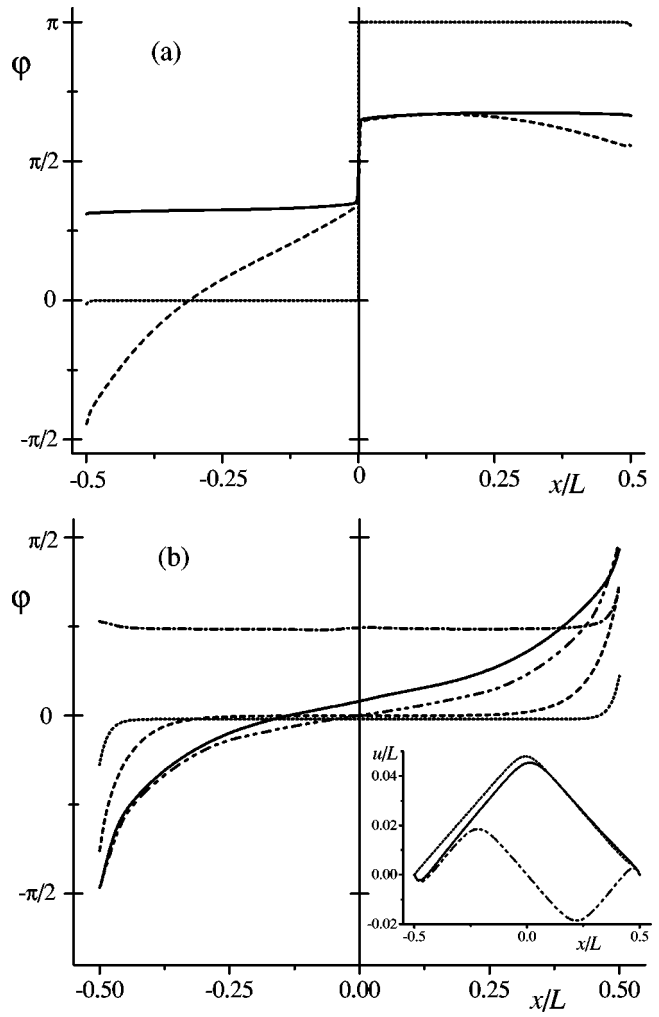

FIG. 2. Spatial variation of φ in the possible stable structures. (a) Common parameters, $r=0.5$, $\gamma_{np}=0$. Solid line, uniform B ($k_S=10^{-1}, \gamma_p=0.01$); dashed line, splayed B ($k_S=10^{-1}, \gamma_p=1$); dotted line, V_h ($k_S=10^{-4}, \gamma_p=1$). (b) Common parameters, $r=0.2$, $\gamma_{np}=5$. Solid line, S ($k_S=10^{-1}, \gamma_p=2$); dash-dot-dotted line, S^d ($k_S=10^{-1}, \gamma_p=2$); dashed line, S ($k_S=10^{-2}, \gamma_p=2$); dotted line, S ($k_S=10^{-3}, \gamma_p=2$); dash-dotted line, B_φ ($k_S=10^{-3}$, $\gamma_p=1$). The inset shows some of the corresponding spatial variations of the layer displacement u.

the same effect in the chevron geometry of smectic layers. Their model is built on earlier work of Nakagawa [20,21]. Their study includes only the effects of rather low spontaneous polarization (up to 60 nC/cm^2) on the B structure with $r=0.89$.

The electrostatic self-interaction, however, prefers a monostable structure in which $\varphi=0$ throughout the cell. In comparison to a B structure a monostable structure is accompanied by a larger splay deformation in the nematic director around the chevron tip. Across the chevron tip the layer tilt changes from δ_E to $-\delta_E$. The x component of the director changes from $\sin(\vartheta_B-\delta_E)$ to $\sin(\vartheta_B+\delta_E)$. The lower the equilibrium layer tilt the cheaper is this splay deformation. So we expect that lowering of the ratio $r=\delta_E/\vartheta_B$ promotes the stability of the monostable structure. Another candidate for a monostable structure is the one with $\varphi=0$ on one side of the chevron tip and $\varphi=\pi$ on the other side [dotted line in Fig. 2(a)]. In this case the x component of the director changes from $-\sin(\vartheta_B-\delta_E)$ to $\sin(\vartheta_B-\delta_E)$ across the chevron tip. If $\delta_E\approx\vartheta_B$ the splay deformation is negligible. Nevertheless, even at $r=1$, this structure is energetically very expensive because the cone angle at the chevron tip reduces to zero. This structure we call V_h, where V stands for V-shaped and h for high, meaning that the structure has very high energy. The structure is metastable at high values of the spontaneous polarization ($P_S>100$ nC/cm^2 at the chosen set of typical parameters).

Since the director tilt out of the xz plane is preferred at the chevron tip in order to reduce the nematic deformation, we find that there are no perfectly monostable structures in the chevron SSFLC cells. The director is always tilted in the yz plane, although this tilt is negligibly small in a large range of the surface anchoring strength, stiffness parameter and also at quite high ratios between the equilibrium layer tilt and the cone angle as we shall show in the following section. According to the results obtained in the bookshelf geometry [12], structures with $\varphi<0.1$ throughout the cell would exhibit V-shaped switching. We expect that it is the same in the chevron geometry of the smectic layers. So in the structure diagrams shown in the following section we shadow the region where structures with $\varphi<0.1$ exist.

Even if $\varphi\approx0$ inside the cell, the director tilt out of the xz plane can be significant close to the surfaces in a region of thickness λ_S due to the polar surface anchoring. In Fig. 2(b) we show typical spatial variation of φ in such cells. The splayed variation of φ in the S structure at high k_S (solid line, $k_S=10^{-1}$) becomes uniform with $\varphi\approx0$ inside the cell at low k_S (dashed and dotted line, $k_S=10^{-2}$ and $k_S=10^{-3}$, respectively). Because of that we denote all these structures by S.

In general, the B structures always switch with a threshold and the S structures have the possibility to exhibit V-shaped switching if $\varphi\approx0$ in most of the cell. In that case we call the S structure monostable or quasimonostable to keep in mind that $\varphi(x)$ is not exactly zero.

At $\gamma_p<\gamma_{np}$ there can also exist a structure which is intermediate between the S structure (with φ at the chevron tip being close to zero) and the B structure (with φ at the chevron tip being $\pm\pi/2$). We call this structure a B_φ structure and its spatial dependence of φ is shown by a dash-dotted line in Fig. 2(b).

At the surfaces the director position on the cone is a function of the strength of the surface anchoring. Let us suppose that the model would not allow for layer deformations. Then the only possibility to accommodate the requirements of the surface is the one shown in Fig. 3(a), where the director position on the cone close to the left surface is shown for the structure where $\varphi=0$ far from the surface and $\varphi=-\pi/2$ at the surface (very strong polar anchoring). Such spatial variation of the director position on the cone is accompanied by a strong deformation in the nematic director. This is shown by the arrows above the smectic cones: the x component of the director changes the sign on approaching the surface, while the y component increases. Another possibility is to bend the smectic layers [Fig. 3(b)]. In this case the splay deformation in the director reduces, however the price is paid by the

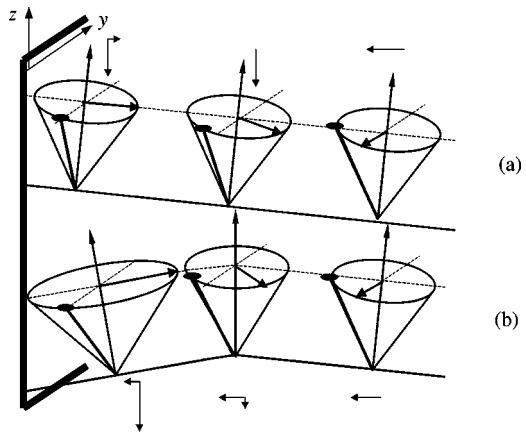

FIG. 3. Spatial variation of the director position on the cone close to the left surface in the case of strong polar surface anchoring. The director rotation on the cone from $\varphi \approx 0$ in the bulk to $\varphi \approx -\pi/2$ at the surface can be achieved by (a) a splay deformation in the nematic director or (b) bending of the smectic layers. The arrows above/below the smectic cones present the x (horizontal arrows) and the y (vertical arrows) components of the nematic director.

deformation due to the layer bending. In addition we must consider that the surface electroclinic effect will tend to increase the cone angle at the surface. The resulting stress is also relieved by layer bending. So we expect to have the situation depicted in Fig. 3(b), especially at low r.

Close to the right surface the situation is similar [see Fig. 4(a)]. Here the nematic deformation can in principle be reduced by increasing the layer tilt and as long as the surface anchoring is not too strong or/and the magnitude of the spontaneous polarization is not too large our model actually predicts such a situation. However in the case shown in Fig. 4(a), the anchoring is very strong. In this case the surface electroclinic effect is large which additionally increases the nematic deformation and again bending of the layers as shown in Fig. 4(b) occurs in order to relieve the stress.

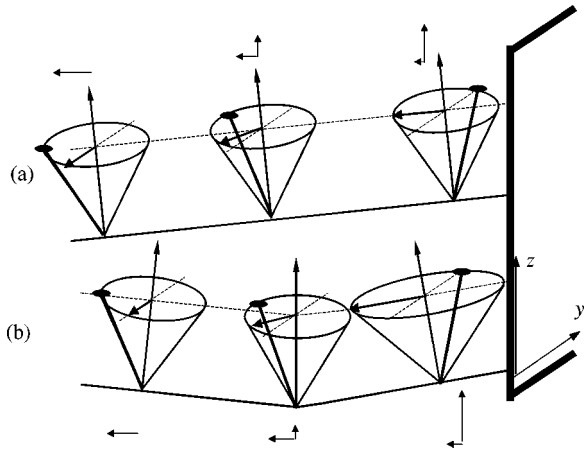

FIG. 4. Spatial variation of the director position on the cone close to the right surface in the case of strong polar surface anchoring. The director rotation on the cone is achieved (a) by a splay deformation in the nematic director or (b) by bending of the smectic layers. The arrows above/below the smectic cones present the x-(horizontal arrows) and the y (vertical arrows) components of the nematic director.

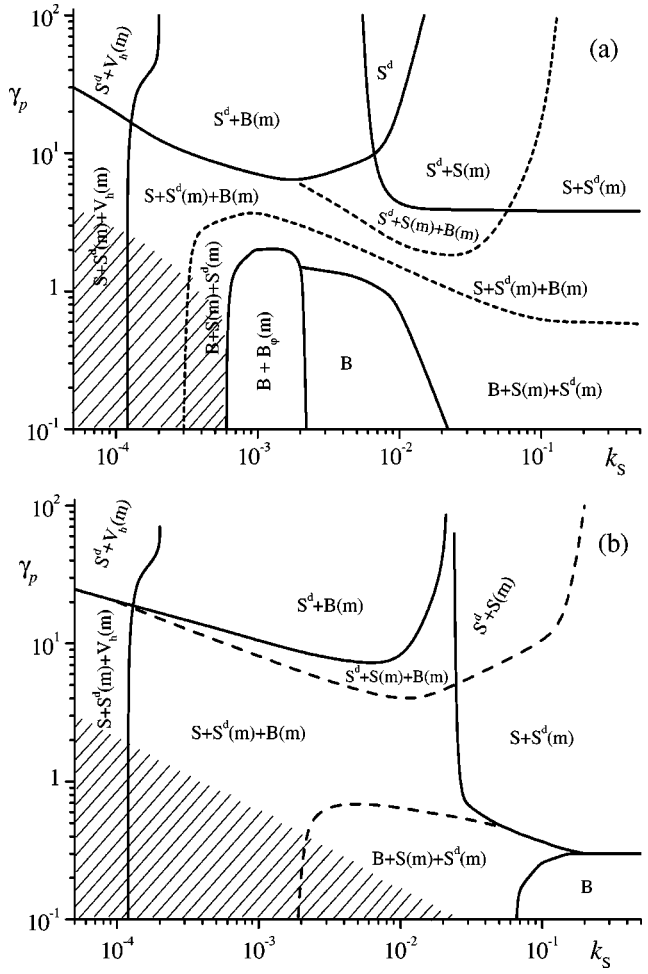

FIG. 5. Stability diagram of the structures vs polar anchoring (γ_p) and the stiffness parameter (k_S) at $\vartheta_B = 30°$, $r = 0.2$ and (a) $\gamma_{np} = 5$ and (b) $\gamma_{np} = 0$. $S(m)$, $B(m)$, $V_h(m)$, and $S^d(m)$ designate metastable structures. Solid curves are the limits of stability of certain structures and the dashed curves show where the enthalpies of the two structures are the same. If there are two metastable structures the one with the highest energy is written last. In the shaded region the value of φ in the S structure is lower than 0.1 throughout the cell.

Bending of layers at the surfaces is in the opposite direction [compare Figs. 3(b) and 4(b)]. Such layer bending at the surfaces can be accommodated only by a double chevron structure inside the cell [see the spatial dependence $u(x)$ for the double chevron in Fig. 2(b)]. The double chevron structure we denote by S^d. In the following section we show that the double chevron structure is stable at strong polar anchoring. Due to the surface electroclinic effect it is metastable also at weak polar anchoring.

IV. RESULTS AND DISCUSSION

In Fig. 5 we show the structure diagram for a material with $\vartheta_B = 30°$ and $r = 0.2$. Together with the set of param-

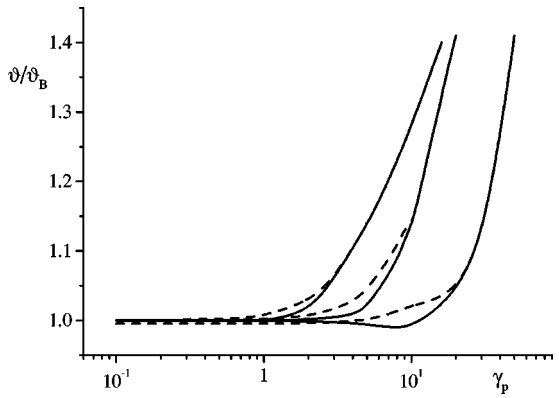

FIG. 6. The value of ϑ at the left (solid lines) and the right (dashed lines) surfaces as a function of polar anchoring (γ_p) at $\gamma_{np}=0$ and $r=0.2$. From left to right: $k_S=10^{-2}$, $k_S=10^{-3}$, and $k_S=10^{-4}$.

eters mentioned in Sec. II A and $k_S\sim10^{-5}$ this would be the parameters which correspond to W415. We studied the possible structures as a function of the stiffness parameter k_S and the strength of the polar surface anchoring γ_p. For the value of the nonpolar anchoring we choose a typical value which is $W_{np}=10^{-5}$ J/m^2 and then $\gamma_{np}=5$ [Fig. 5(a)]. In Fig. 5(b) we show the same type of the structure diagram at zero nonpolar anchoring. The system shows a surprising number of stable structures, accompanied by one or two metastable ones, denoted by *m*.

At low magnitudes of the spontaneous polarization ($k_S>10^{-2}$) both *B* and *S* structures coexist at $\gamma_p<\gamma_{np}$ as suggested by the discussion in Sec. II. At $\gamma_p>\gamma_{np}$ only the splayed structure is stable, but it becomes metastable with respect to a double chevron structure due to the surface electroclinic effect. The magnitude of the surface electroclinic effect, i.e., the value of ϑ at the surface at several values of k_S as a function of the surface anchoring strength (γ_p) is shown in Fig. 6. The cone angle at the surface increases significantly at strong polar surface anchorings. At larger values of the spontaneous polarization stronger surface anchoring is required for the same increase of ϑ. The dependence is approximately the same at all *r* and all γ_{np}, both in the *S* and the *B* structures.

At higher magnitudes of the spontaneous polarization ($k_S<10^{-2}$) the thickness of the surface deformed layer is so small that it does not affect the structure of the chevron tip. To relax the nematic deformation $\varphi\approx\pm\pi/2$ is preferred around the chevron tip, so the *B* structure is metastable also at $\gamma_p>\gamma_{np}$. At low γ_p the compound effect of the nonpolar surface anchoring and the nonpolar ''anchoring'' at the chevron tip even pushes out the splayed structure completely.

The presence of nonpolar anchoring enforces the stability of the *B* structure at $\gamma_p<\gamma_{np}$. This can be seen by a comparison of the structure diagrams in Fig. 5(a) ($\gamma_{np}=5$) and in Fig. 5(b) ($\gamma_{np}=0$). In the case of $\gamma_{np}=0$ the area in which the *S* structure is stable enlarges and it is pushed towards lower magnitudes of the spontaneous polarization (higher k_S). However, even at $\gamma_{np}=0$, the *B* structure is stable at low k_S and at low γ_p and the *S* structure is stable at higher γ_p. This is due to the nonpolar anchoring behavior of the chevron tip. We can estimate that the effective strength of the nonpolar anchoring at the chevron tip is ≈0.3 and the corresponding anchoring strength is thus 6×10^{-7} J/m^2.

In the shaded region in the structure diagrams the value of φ in the *S* structure is lower than 0.1 everywhere in the cell. In a bookshelf geometry such a structure would exhibit V-shaped switching [12], so we presume it is the same in the chevron geometry. From the structure diagram we also deduce that at the parameters typical for the W415 liquid crystal ($k_S=10^{-5}$) and the typical values of the surface anchoring ($\gamma_p=\gamma_{np}=5$), the structure is practically monostable with $\varphi\approx0$ everywhere in the cell.

At $k_S<10^{-2}$ the value of φ inside the cell is already close to zero [see the dashed line in Fig. 2(b)]. At $k_S<10^{-3}$ the thickness of the surface deformed layer (the region where the effect of the surface anchoring is felt), where φ can be significantly different from zero, is only 3% of the cell thickness. In this case the structure can probably be expected to exhibit V-shaped switching. A more detailed study of the electro-optical response of the *S* structures is needed, however, to find out the maximum width of the surface deformed layer such that the structures still switch without threshold.

The *B* structure is (meta)stable only at $k_S>10^{-4}$. At lower k_S the high-energy V_h structure and the, practically monostable, *S* structure exist. This agrees with the argument presented in Sec. II that at $k_S\sin^2\vartheta_B<k_{\|,ch}$ monostable structure can be expected, because the electrostatic contribution to the free energy is larger than the nematic and smectic contributions. This argument is valid at all *r* and γ_p which was also confirmed by the numerical calculations.

If $k_S>10^{-4}$, then the monostable *S* structure is pushed towards lower k_S by increasing *r*. This is expected, because the splayed deformation around the chevron tip in the *S* structure increases with increased ratio *r* as discussed in Sec. III. Also, at larger *r* a double chevron structure is stable at stronger polar anchoring, because layer bending is more energetically expensive at higher δ. Let us also point out that due to the surface electroclinic effect the double chevron structure S^d is metastable wherever *S* is (meta)stable. We have also checked for the stability of the triple and even higher chevron structures. Regardless of the number of chevron peaks in the initial approximation the structure always relaxes into a single or a double chevron structure.

Finally, we have also considered the effect of the thickness *a* of the insulating alignment layer on the structure. The results obtained in the bookshelf geometry [12] are valid here as well. In general the value of φ inside the cell is reduced if *a* increases, so thicker surface insulating layers drive the system into the monostable state, as predicted by Clark *et al.* [9].

V. CONCLUSIONS

We have studied theoretically the director and layer structure in surface stabilized ferroelectric liquid crystal cells. The model put forward by the present authors and co-workers in [13] was used and modified so that it is applicable to the systems with spontaneous polarization. We also introduced additional parameter $r=\delta_E/\vartheta_B$ into the model which en-

abled us to study chevrons with different ratios between the equilibrium layer tilt and the smectic cone angle. We considered the effects of the magnitude of the spontaneous polarization, thickness of the insulating alignment layer, the strength of the polar and nonpolar surface anchoring and the ratio r on the director and layer structure. Due to the numerous competing effects in the SSFLC cells the system shows a number of stable structures, accompanied by one or two metastable ones.

At magnitudes of the spontaneous polarization larger than the critical value ($P_S^{cr}=100$ nC/cm^2 at the typical set of parameters chosen in the present paper) the electrostatic contribution to the free energy is larger than the nematic and smectic contributions. In this case only practically monostable structures exist with $\varphi\approx 0$ inside the cell. In a region of thickness λ_S close to the surface the angle φ may differ significantly from zero due to the surface anchoring. At $P_S<P_S^{cr}$ both bistable and quasimonostable structures can coexist. The general rule is that the system is driven into the monostable state if (a) the magnitude of the spontaneous polarization increases, (b) the ratio r reduces, (c) the thickness of the insulating alignment layer increases, and (d) the strength of the polar surface anchoring increases with respect to the nonpolar one.

Polar surface anchoring induces a large surface electroclinic effect. As a result the nematic deformations close to the surfaces are very strong and the stress is relieved by bending of the smectic layers. This leads to the formation of a double chevron structure which is stable at very large polar anchoring. Due to the surface electroclinic effect it is metastable also at lower values of the polar anchoring.

To conclude, we have shown that structures which can be expected to exhibit V-shaped switching exist also in the SSFLC cells with the chevron geometry of the smectic layers. In a broader context, our results which suggest an abundance of stable and metastable structures, could perhaps help to explain the richness of the textures observed in systems with high magnitudes of the spontaneous polarization.

ACKNOWLEDGMENT

This work was partially supported by Grant No. Z1-3292 of the Slovenian Ministry of Education, Science, and Sport.

[1] T.P. Rieker, N.A. Clark, G.S. Smith, D.S. Parmar, E.B. Sirota, and C.R. Safinya, Phys. Rev. Lett. **59**, 2658 (1987).
[2] Y. Ouchi, J. Lee, H. Takezoe, A. Fukuda, K. Kondo, T. Kitamura, and A. Mukoh, Jpn. J. Appl. Phys., Part 1 **27**, L725 (1988).
[3] N. Vaupotič, V. Grubelnik, and M. Čopič, Phys. Rev. E **62**, 2317 (2000).
[4] N. Hayashi, T. Kato, T. Ando, A. Fukuda, S. Kawada, and S. Kondoh, Phys. Rev. E **68**, 011702 (2003).
[5] L.M. Blinov, E.P. Pozhidaev, F.V. Podgornov, S.A. Pikin, S.P. Palto, A. Sinha, A. Yasuda, S. Hashimoto, and W. Haase, Phys. Rev. E **66**, 021701 (2002).
[6] S. Inui, N. Imura, T. Suzuku, H. Iwane, K. Miyachi, Y. Takaishi, and A. Fukuda, J. Mater. Chem. **6**, 671 (1996).
[7] N.J. Mottram and S.J. Elston, Liq. Cryst. **26**, 1853 (1999).
[8] N.J. Mottram and S.J. Elston, Phys. Rev. E **62**, 6787 (2000).
[9] N.A. Clark, J.E. Maclennan, R. Shao, D. Coleman, S. Bardon, T. Bellini, D.R. Link, G. Natale, M.A. Glaser, D.M. Walba, M.D. Wand, X.H. Chen, P. Rudquist, J.P.F. Lagerwall, M. Buivydas, F. Gouda, and S.T. Lagerwall, J. Mater. Chem. **9**, 1257 (1999).
[10] N.A. Clark, D. Coleman, and J.E. Maclennan, Liq. Cryst. **27**, 985 (2000).
[11] B. Park, S. Seomun, M. Nakata, M. Takanishi, Y. Takanishi, and H. Takezoe, Jpn. J. Appl. Phys., Part 1 **38**, 1474 (1999).
[12] M. Čopič, J.E. Maclennan, and N.A. Clark, Phys. Rev. E **65**, 021708 (2002).
[13] N. Vaupotič, S. Kralj, M. Čopič, and T.J. Sluckin, Phys. Rev. E **54**, 3783 (1996).
[14] R.F. Shao, J.E. Maclennan, N.A. Clark, D.J. Dyer, and D.M. Walba, Liq. Cryst. **28**, 117 (2001).
[15] J. Xue and N.A. Clark, Phys. Rev. Lett. **64**, 307 (1990).
[16] W.H. Press, B.P. Flannery, S.A. Teukolsky, and W.T. Vetterling, *Numerical Recipes* (Cambridge University Press, Cambridge, 1986).
[17] M. Cagnon and G. Durand, Phys. Rev. Lett. **70**, 2742 (1993).
[18] M. Nakagawa and T. Akahane, J. Phys. Soc. Jpn. **55**, 1516 (1986).
[19] J. Sabater, J.M.S. Pena, and J.M. Otón, J. Appl. Phys. **77**, 3023 (1995).
[20] M. Nakagawa, Displays **11**, 67 (1990).
[21] M. Nakagawa, Liq. Cryst. **14**, 1763 (1993).